REVIEW
ARTICLE

KIMIKA Volume 34, Number 2, pp. 61-86 (2023)
 ISSN 2508-0911
https://doi.org/10.26534/kimika.v34i2.61-86

The Role of Molecular Dynamics Simulations in Elucidating Interactions between Antimicrobial Peptides and Model Biological Membranes

Searle Aichelle S. Duay*

Department of Chemistry, De La Salle University, 2401, Taft Ave., Malate, Manila, Philippines 0922

*Author to whom correspondence should be addressed; email: searle.duay@dlsu.edu.ph

ABSTRACT

In addressing the global problem of antimicrobial resistance, an emerging class of molecules called antimicrobial peptides (AMPs) are being widely studied. Their interactions with cell membranes are instrumental in their killing action, usually by forming pores or translocating to act on an internal target. Molecular dynamics (MD) simulations have played an essential role in understanding the atomistic mechanisms of such interactions. This review will highlight key findings from various MD studies, such as the formation of nanoaggregates and different types of pores. We will also discuss the role of selecting the membrane model composition, the level of detail in the simulation, and the choice of force field. It is evident in this review that our understanding of the interactions of AMPs and membranes has grown over the recent years through the help of MD simulations. Still, remaining concerns in MD studies of such systems must be addressed to gain more information.

Keywords: *antimicrobial peptides; molecular dynamics simulations; peptide-membrane systems*

INTRODUCTION

Antimicrobial resistance (AMR) is a pressing global public health problem wherein microbes, such as bacteria and viruses, develop resistance against antimicrobial drugs. The World Health Organization considers it one of the top ten global health threats (World Health Organization, n.d.). The continuing problem of antimicrobial resistance pushed the field of drug discovery towards looking for new antimicrobial substances. A significant group of pathogens called ESKAPE (*Enterococcus faecium, Staphylococcus aureus, Klebsiella pneumoniae, Acetinobacter baumannii, Pseudomonas aeruginosa,* and *Enterobacter spp.*) was seen to be familiar sources of nosocomial infections in many immunocompromised patients (Rice, Federal, 2008). These pathogens have also developed various antimicrobial resistance mechanisms (Rice, Progress,

2010). In addressing this issue over the years, peptides that were seen to have antimicrobial activity against a broad spectrum of pathogens were studied and developed.

Antimicrobial peptides (AMPs) are short sequences of amino acids, usually in the range of 20 to 100 amino acids, produced by most organisms as part of their natural immunity (Conklin et al., 2017; Fjell et al., 2012). They serve as the first line of defense against pathogenic microbes and are known to kill bacteria via membrane disruption or to act on an intracellular target to inhibit necessary biochemical pathways (Balandin and Ovchinnikova, 2016; Juliano et al., 2017; Libardo et al., 2017). They are also considered intrinsically disordered peptides as their usual short length does not allow them to form thermodynamically stable structures in solution (Zasloff, 2002). These characteristics of AMPs will enable them to be good alternatives to much more studied small molecule antibiotics, if not improvements. Their ability to not be restricted to a specific conformation gives rise to multiple mechanisms of action against microbes (Lai and Gallo, 2009). AMPs may vary in conformation in response to the changes brought by the resistance mechanism of the microbes. In addition to this benefit, the expression of extremely high concentrations of AMPs *in vivo* may be complicated for the microbe to develop a resistance mechanism against it (Ghosh et al., 2002). There is also an expensive tradeoff between maintaining the integrity of the cell membrane and varying the membrane composition to prevent AMPs from disrupting the membrane (Lai and Gallo, 2009; Zasloff, 2002). These factors are crucial in addressing the global problem of antimicrobial resistance.

A critical aspect of studying biochemical processes, especially in drug development, is the interaction of a molecule with the first line of defense of the cell – its lipid membrane. Biological membranes are complex systems in that aside from being composed of various types of lipids, some proteins and carbohydrates are present in the sea of dynamic fatty acid esters. Whether AMPs act via membrane disruption or action on an internal target, the peptides still have to interact with the cell membrane. Understanding the membrane properties of the target pathogens is essential in designing AMPs. For example, cationic AMPs are active against Gram-negative opportunistic bacteria as the outer membrane of these pathogens contains anionic lipopolysaccharides (LPS) (Bhattacharjya and Straus, 2020).

Currently, there are three known membranolytic mechanisms of AMPs: barrel-stave pore formation (Ehrenstein and Lecar, 1977), toroidal pore formation (Ludtke et al., 1996; Wimley, 2010), and carpet model (Lee et al., Antimicrobial, 2016; Shai, 1999). Experimental studies such as confocal fluorescence microscopy (Zakharova et al., 2022), electron microscopy (Koike M et al., 1969), insertion experiments in monolayers (Clausell et al., 2007), and X-ray diffraction (Juliano et al., 2020) have been used extensively to study the interactions of AMPs with different membrane models and cell membranes. However, the available experimental methods cannot capture the atomistic level of mechanistic details about the process of peptide attraction to and insertion into the membrane. Understanding the role of specific amino acids and their relative positions in the sequence may help us further design AMPs capable of having multiple mechanisms of action.

Molecular dynamics (MD) simulations have been an essential tool in studying interactions between biological systems such as protein-DNA (Yoo et al., 2020), small molecules, and enzymes (Gharaghani et al., 2013; Pan et al., 2021; Shi et al., 2020), and carbohydrate-protein (Fadda and Woods, 2010). Most importantly for this review, it has been utilized in many AMP-membrane studies to elucidate the peptide's mechanism further. A recent review paper by de la Fuente-Nuñez et al. highlighted the importance of MD simulations in AMP discovery (Palmer et al., 2021). A typical MD simulation employs a force field that contains parameters for bonded and non-bonded interactions between atoms. Given an initial structure of the system that includes the initial coordinates of every atom, their energies are calculated, followed by a series of integration steps to predict the next spatial coordinates of every atom after one defined timestep. This will be iterated multiple times until the desired simulation time is achieved.

In designing MD simulations, one must consider the required timescale to observe the process of interest thoroughly. For example, we do not expect proteins to fold from a denatured state to their native state in the microsecond timescale. Previously, it was seen that slow orientational and conformational fluctuations require microsecond timescales for sufficient sampling and agreement between simulation data and experimental data (Wang et al., How, 2014). Millisecond-long simulations have been done already, but the physical time required to run such simulations varies depending on the size of the system, the level of details in the model (atomistic or coarse-grained), and the computational capability of computer nodes where the simulations will run, among others. In addition, physical transitions that require more than one k_BT (where k_B is the Boltzmann constant and T is absolute temperature) will be challenging to observe, leading to poor system sampling. To overcome these problems, enhanced sampling techniques for MD simulations were developed. In these methods, bias forces are usually added to compel the system to undergo the desired transition and explore a much larger configurational space. Recently, a review article on enhanced sampling methods was published (Hénin et al., 2022), which can serve as a guide for readers who want to understand the techniques discussed here further.

This review article will explore studies that provide insights into the interaction of AMPs with model membranes through the lens of molecular dynamics simulations. A review of MD simulations of cell-penetrating peptides (CPPs) was recently published (Ouyang et al., 2022). While CPPs and AMPs are known to belong to the group of membrane-active peptides, the membranolytic mechanisms of AMPs open up a lot of possible MD investigations that can be done on peptide-membrane systems. We will also look at standard practices, the latest MD methodologies, and problems that need addressing in the field.

DIFFERENT COMPOSITIONS OF MODEL MEMBRANES

While antimicrobial peptides cater to many microbes, including viruses and fungi, most MD studies on AMPs focus on those with antibacterial activity. Gram-negative bacteria have two distinct cell membranes – the outer and inner membranes – separated by periplasm and a thin cell wall. In contrast, Gram-positive bacteria have a cytoplasmic cell membrane and a thick cell wall of multiple peptidoglycan layers (Sohlenkamp and Geiger, 2016). Each membrane has a unique lipid composition that varies across different bacterial species. In the Gram-negative outer membrane (OM), the outer leaflet usually comprises lipopolysaccharides (LPS) (Duong et al., 1997). The inner leaflet is majorly made up of phosphatidylglycerols (PGs) and phosphatidylethanolamines (PEs) with a few cardiolipin (CL) molecules (Willdigg and Helmann, 2021). The Gram-negative inner membrane (IM) usually has the same composition as the inner leaflet of the outer membrane (Silhavy et al., 2010). For Gram-positive bacteria, the cytoplasmic membrane mainly comprises PGs and cardiolipin, with some species having PEs in the mix (Rajagopal and Walker, 2017). A striking feature of the Gram-positive cell envelope is the thick peptidoglycan layer, ranging from 30 to 100 nm (Silhavy et al., 2010). Due to the scope of this review, we will not be discussing the subtle differences in the lipid composition of cell membranes across different bacteria. A recent review paper by Sohlenkamp and Geiger can be read for an extensive discussion (Sohlenkamp and Geiger, 2016). A summary of the details from the unbiased simulation studies covered in this review is in Table 1.

Table 1. Systems of AMP-model membrane unbiased simulations included in this review.

Antimicrobial Peptide (Net charge at pH 7)	Model Membrane Composition	Force Field (Resolution)[1]	Average Simulation Time	Reference
Polymyxin B (+5)	Inner Membrane (both outer and inner leaflet): 75% PE, 20% PG, 5% Cardiolipin Outer Membrane Outer Leaflet: Pure Re LPS Outer Membrane Inner Leaflet: 90% PE, 5% PG, 5% cardiolipin Pure Lipid A bilayer	MARTINI (CG) GROMOS 53A6 for the peptide and LPS (UA) GROMOS-CKP for the phospholipids (UA)	557.5 ns for the inner membrane 450 ns for the outer membrane	(Berglund et al., 2015)
	Pure Re LPS	MARTINI (CG)	5 μs	(Jefferies et al., 2017)
	Inner Membrane (both outer and inner leaflet): 75% PE, 25% PG Outer Membrane (both outer and inner leaflet): Pure Re LPS	MARTINI (CG)	1 μs for the inner membrane 3 μs for the outer membrane	(Fu et al., 2020)
	Inner Membrane (both outer and inner leaflet): 80% PE, 16% PG, 4% Cardiolipin Outer Membrane Outer Leaflet: Pure Re LPS or Pure Lipid A or 80% Re LPS, 20% PE/PG or 20% Re LPS, 80% PE/PG Outer Membrane Inner Leaflet: 80% PE, 16% PG, 4% Cardiolipin	MARTINI (CG)	10 μs	(Sun et al., Interactions, 2022)
B2088 (+12) $(RGRKVVRR)_2KK$	Mammalian Membrane: Pure PC Bacterial Membrane: 75% PE, 25% PG	CHARMM27 for peptides (AA) CHARMM36 for lipids (AA)	200 ns	(Li et al., 2013)
CM15 (+6) KWKLFKKIGAVLKVL-NH_2	Pure PC Pure PG 1:2 PG:PC	CHARMM27 for peptides (AA) CHARMM36 for lipids (AA)	116 ns	(Wang et al., Comparative, 2012)
LL-37 (+6)	Mammalian Membrane: Pure PC Bacterial Membrane: Pure PG	GROMOS53A6 (UA)	667 ns	(Zhao et al., 2018)
BMAP27 (+10)	Pure PC Pure PG Pure PS	MARTINI (CG) AMBER99SB-ILDN for peptides (AA) Slipid/AMBER for lipids (AA)	337.5 ns for atomistic 10 μs for coarse-grained	(Sahoo and Fujiwara, 2016)

Antimicrobial Peptide (Net charge at pH 7)	Model Membrane Composition	Force Field (Resolution)[1]	Average Simulation Time	Reference
Clavanin (+4)	80% PE, 20% PG	CHARMM36 (AA)	500 ns	(Duay et al., 2019)
Melittin (+5)	Pure PC	MARTINI (CG)	2.97 μs	(Santo and Berkowitz, 2012)
	70% PC, 30% PG	MARTINI (CG) GROMOS96 53a6 (UA)	1 μs for coarse-grained 50 ns for united atom	(Santo et al., 2013)
	Pure PC	CHARMM (AA) MARTINI (CG)	400 ns for atomistic 1200 ns for coarse-grained	(Sun et al., Multistep, 2015)
	70% PC, 30% PG	MARTINI (CG) CHARMM36M (AA)	300 ns for atomistic 5 μs for coarse-grained	(Sun et al., Organization, 2022)
	Pure PC	pSPICA (CG)	5 μs	(Miyazaki and Shinoda, 2022)
Myxinidin (+2) WMR (+5)	80% PE, 20% PG 65% PE, 23% PG, 12% CL	CHARMM36M for peptides (AA) CHARMM36 for lipids (AA)	5 μs	(Cherniavskyi et al., 2024)
Magainin-2	Pure PC	MARTINI (CG)	4.88 μs	(Santo and Berkowitz, 2012)

[1] All-atom simulations are written as AA; United-atom simulations are written as UA; Coarse-grained simulations are written as CG

In a study by Berglund and coworkers, they comprehensively studied the interaction of AMP polymyxin B (PmB) with different model membranes of Gram-negative bacteria (Berglund et al., 2015). The approach was to conduct separate simulations for a more realistic model of the OM (composed of Re LPS in the outer leaflet and a mixture of PE, PG, and CL in the inner leaflet), a simplified model of the OM (composed of pure Lipid A), and an IM model (consisting of a mixture of PE, PG, and CL). In this OM model, there was an initial approach by the peptide due to the favorable hydrogen bonding interactions between the polar α, γ-diamino butyric acid (DAB) residues of the peptide and the sugars of Re LPS. However, no further insertion was observed in the timescale of the study. In addition to the initial membrane insertion, aggregation of PmB in a micellar structure was also seen. Doing steered simulations to pull the peptide further into the OM did not result in peptide insertion. It is worth noting that the Re LPS molecules were modeled atomistically, thus requiring more extensive computational power to run longer simulation timescales. The need for a simplified model of the OM arose from the inability of PmB to penetrate the membrane in the chosen timescale of the study due to the slow dynamics of LPS. The difference in this simplified model from the asymmetric model earlier is the lack of sugars. Due to this, the peptide overcame the barrier from hydrogen bonding interactions with the sugars. The polar DAB residues, instead, interacted with the phosphates and intermittently displaced the Mg^{2+} cations, destabilizing the simplified outer membrane model.

Latter simulation studies took advantage of the coarse-grained LPS models to achieve longer timescales of interaction with PmB (Fu et al., 2020; Sun et al., Interactions, 2022). Timescales

achieving 10 μs of simulation with Re LPS allowed observation of preferential interaction of PmB to LPS after its binding (Sun et al., Interactions, 2022). However, similar to the atomistic simulations, further insertion of the peptide to a pure LPS outer membrane was inhibited by the sugars in the LPS. Even with longer timescales, the peptide insertion cannot be observed, hinting at a more complex PmB insertion mechanism into the OM. Changing the OM lipid composition into a mixed structure of LPS and phospholipids resulted in the insertion of PmB into the model membrane (Sun et al., Interactions, 2022). The mean distance between PmB and the bilayer center in the inserted models is about 1.1 nm, while for those that did not insert, the mean distance is about 3.0 nm. Regarding preferential interaction, the affinity towards LPS developed only in OM systems where only 20% of the lipids are LPS (Sun et al., Interactions, 2022). The preferential interaction happened only after the insertion of PmB when its acyl tail had already been inserted into the phospholipid-rich region, demonstrated by the spontaneous accumulation of LPS around the acyl tail. Increasing the proportion to 80% LPS showed no preferential interaction with any lipid type.

The level of information that can be obtained from an atomistic model membrane versus a coarse-grained model membrane can also be demonstrated in IM models. In both atomistic and coarse-grained models, the electrostatic interactions between the DAB residues of PmB and the lipid headgroups drive the peptide binding (Berglund et al., 2015; Fu et al., 2020). In the atomistic model, it was seen that PmB binding and insertion significantly increased the disorder of the lipid acyl tails (Berglund et al., 2015). However, in a longer coarse-grained simulation, it was discovered that PmB eventually fills up the vacancies in lipid packing, which makes the lipid tail more ordered, increasing membrane rigidity and restricting lipid diffusion (Fu et al., 2020).

In contrast with bacterial membranes, mammalian cell membranes contain more neutral lipids. Phosphatidylcholines make up the majority of lipids in mammalian cell membranes. This is followed by phosphatidylethanolamines and phosphatidylserines. The PGs primarily synthesize cardiolipin and bis(monoacylglycerol)phosphate (Cockcroft, 2021). Commonly used model membranes for mammalian cells in MD simulations are majorly comprised of 1-palmitoyl-2-oleoyl-*sn*-glycero-3-phosphocholine (POPC) (Li et al., 2013; Wang et al., Comparative, 2012; Zhao et al., 2018). The neutrality of this model membrane is less preferred by the AMP LL-37 than a purely POPG bilayer (Zhao et al., 2018). The long-range electrostatic interactions between a positively charged peptide and an anionic bilayer allow the peptide to rapidly approach the membrane surface (Li et al., 2013). The helical structures of LL-37 (Zhao et al., 2018) and BMAP27 (Sahoo and Fujiwara, 2016) were also disrupted in a POPC bilayer, contrary to what is observed in a POPG bilayer. While these MD simulation studies agree with experimental results, some MD studies do not support the empirical findings. For example, the AMP CM15 was determined to be non-hemolytic by inhibition zone (Andreu et al., 1992) and leakage assays (Mancheño et al., 1996). However, an MD simulation comparing the interaction of CM15 with bacterial and mammalian model membranes showed no selectivity towards the bacterial membrane (Wang et al., Comparative, 2012). This contradicts the non-hemolytic nature of CM15. It implies that MD simulations alone cannot predict the selectivity of AMPs towards a particular membrane, even if they can sometimes support experimental findings on selectivity. It also suggests that a more realistic model of the mammalian cell membranes might be needed to observe this selectivity.

FORCE FIELDS FOR ANTIMICROBIAL PEPTIDE-MEMBRANE SIMULATIONS

Force fields are a set of parameters and mathematical models that will dictate how atoms (or groups of atoms) will interact and behave in molecular dynamics. The use of different force fields on lipid bilayer systems alone illustrates variations in lipid parameters such as ordering and lateral diffusion coefficient (Poger and Mark, 2012). It is, therefore, intuitive that the force fields

that will be applied to the peptides and lipids will also affect their dynamics and interactions with each other. The model resolution (all-atom, united atom, or coarse-grained) and the applicable force fields will depend on the study questions or the motions one would want to observe. For more detailed simulations where interactions between specific atoms are of interest, all-atom (AA) force fields such as CHARMM (Chemistry at HARvard Macromolecular Mechanics) (Best et al., 2012; Feller et al., 1997; Huang et al., 2017; Klauda et al., 2010; MacKerell et al., All-Atom, 1998; Mackerell Jr. et al., Extending, 2004; Schlenkrich et al., 1996) may be used. However, AA simulations are more demanding in computational resources than other model resolutions. To achieve greater sampling efficiency and longer simulation times, coarse-grained (CG) simulations may be employed. This, however, will lose the level of atomic resolution in AA simulations.

The most common force field (FF) of choice for CG models of AMP-model membrane systems is the MARTINI (Marrink et al., Coarse, 2004,; Marrink et al., MARTINI, 2007; Vaiwala and Ayappa, 2024) force field. This force field has a 4:1 mapping scheme, wherein a bead represents a combination of four heavy atoms. In the latest MARTINI force field for lipids (Wassenaar et al., 2015), there are 22 bead types, classified into three groups: C for saturated carbon chains, D for carbon chains with *cis* double bond, and T for carbon chains with *trans* double bond. There are only a few studies that used other force fields. such as SDK (Shinoda et al., 2010), ELBA (Orsi and Essex, 2011), and Fat SIRAH (Barrera et al., 2019). We have only seen one published study that used Fat SIRAH in a peptide-membrane simulation. Most of the simulations that use FAT SIRAH are membrane-bound transmembrane protein systems. For SDK, most systems study other membrane structures such as monolayers, bicelles, and vesicles. The Shinoda-DeVane-Klein (SDK) force field was explicitly developed for lipids to reproduce empirical membrane properties such as tension, elasticity, and structure. SPICA is another coarse-grained force field (CG FF) that is an extension of SDK to predict lipid domain formation in membranes, such as those induced by cholesterol (Seo and Shinoda, 2019). The pores formed by melittin in simulations using MARTINI FF were not consistent structurally with experimental observations due to overestimating the membrane line tension. Thus, an extension of SPICA, called pSPICA FF, was developed (Miyazaki and Shinoda, 2022).

For all-atom (AA) force fields, almost all *in silico* studies we have reviewed use the CHARMM force field for both the peptides and lipids. The earliest version of CHARMM that is used in AMP-membrane systems is CHARMM27. Upon the release of CHARMM36 in 2012 and CHARMM36m for proteins in 2016, it has been widely used for AMP-membrane systems. Another AA force field, AMBER (Assisted Model Building with Energy Refinement), is used more in lipid bilayer simulations without antimicrobial peptides. The most recent LIPID21 lipid force field in AMBER has eight types of acyl chains, seven types of headgroups, and cholesterol. There is no apparent reason, however, why AMBER is not used as commonly as CHARMM for AMP-membrane simulations. Furthermore, due to the unavailability of parameters for LPS in AA force fields, AA simulations still need to be done to simulate a more realistic bacterial outer membrane. An option is to use a CHARMM-based all-atom force fields from CHARMM-GUI server (Lee et al., CHARMM-GUI, 2016), but this may require additional parametrization and validation.

An example of a system that highlights the differences in simulation results among different force fields is the pore formation of melittin in a lipid bilayer. When MARTINI FF was used with a nonpolar coarse-grained water model, the peptides did not orient perpendicular to the lipid membrane; thus, a pore was not formed (Santo and Berkowitz, 2012). Modifying the MARTINI FF to use a polarizable CG water model (Yesylevskyy et al., Polarizable, 2010) maintained a transient water channel, made up of four melittin peptides, for the first microsecond of the simulation (Santo et al., 2013). An all-atom model using CHARMM FF could form the same pore but was maintained for a longer simulation time (Sun et al., Multistep, 2015). The same result was obtained when the pSPICA FF was used (Miyazaki and Shinoda, 2022), taking advantage of less computational resources.

At this point, we have seen only two studies that directly compared different force fields (CHARMM27, OPLS-AA/UA, and GROMOS96-53a6) in terms of their accuracy in supporting experimental observations (Bennett et al., 2016; Wang et al., How, 2014). In one study, the helicity of the peptides as they interact with the membrane is more consistent with the NMR results when CHARMM27 is used (Wang et al., How, 2014). Unfolding of the peptides was observed in OPLS-UA simulations, which does not support the empirical data. UA force fields have greater protein flexibility, which could explain the quick unfolding process (Wang et al., How, 2014). In another study evaluating the free energy against pore formation in a PC membrane using different force fields, it was seen that the united-atom Berger lipid parameters had the largest deviation from those that were obtained from the all-atom CHARMM36 and SLipids force fields (Bennett et al., 2016). Other studies involving the GROMOS UA force field exhibit an improbably low energy barrier of melittin-induced pore formation (Irudayam and Berkowitz, 2012; Sengupta et al., 2008). This emphasizes how all-atom and united-atom force fields produce significantly different results when evaluating free energy processes involving AMPs and membrane systems. More studies must be conducted to compare the different types of force fields for AMP-membrane simulations, especially when force field developments are still ongoing. Additionally, the huge differences in observations among different force fields highlight the importance of choosing a more appropriate force field when conducting AMP-membrane simulations.

PEPTIDE INSERTION AND TRANSLOCATION

For a peptide to be inserted and translocated across a membrane, two general steps govern the whole process: peptide approach to the membrane and interaction with the thick hydrophobic membrane core during translocation. These must be taken into consideration when designing membrane-active peptides. During the peptide approach, favorable interactions between the peptide and the hydrophilic surface of the bilayer must be present. Bacterial membranes have a significant amount of anionic POPG; thus, having more cationic residues in peptides is conceptually more advantageous. For example, as discussed earlier, the presence of DAB residues in polymyxin B allows this peptide to promote contact with the negatively charged lipid headgroups of an inner membrane model (Berglund et al., 2015). A later study showed that the same favorable electrostatic interactions were witnessed in a realistic outer membrane model of Re-LPS (Fu et al., 2022). DAB contains a positively charged amine, which is electrostatically attracted to the negatively charged groups of Re-LPS. This lipid is composed of lipid A, which has phosphates, and two to three molecules of 3-deoxy-D-manno-2-octulosonic acid (KDO), which has carboxylates. A three-microsecond-long simulation of PmB with a simplified OM model (composed of only lipid A) showed partial peptide insertion by temporarily displacing Mg^{2+} ions from the lipid phosphates and deforming the membrane locally (Berglund et al., 2015). When observed in longer coarse-grained simulation times in the presence of Na^{+} and Ca^{2+} ions, the DAB residues can displace Na^{+} ions much easier compared to Ca^{2+} ions from the phosphate groups of Re LPS (Jefferies et al., 2017). The full insertion of PmB cannot be observed in the practically accessible unbiased simulation timescales (Jefferies et al., 2017; Mares et al., 2009; Santos et al., 2017; Vesentini et al., 2006).

While the positive charges might influence the peptide approach, the balance between hydrophilic and hydrophobic residues is more significant. In the PMF calculations of a study by Liao et al., melittin, having the second least positive charge and most number of hydrophobic residues among the peptides in their analysis, showed the largest decrease in free energy (Liao et al., 2023). The behavior of peptide as it interacts with the surface of a bacterial model membrane can also change when the former gets protonated, such as due to pH changes. In our previous study, it was seen that increasing the positive charges in the AMP Clavanin A, either by protonating the basic residues or complexing Zn^{2+} ions to the peptide, can induce a shift in preferential interaction of these residues from neutral POPE to anionic POPG (Duay et al., 2019).

Once the peptide is already on the surface of the bilayer, the next challenge is for the peptide to cross the hydrophobic core. A sudden shift in the requirement for a molecule from being charged or hydrophilic to being hydrophobic is a major problem for translocation. Membrane-active peptides address this by being amphipathic and having a mixture of hydrophobic and hydrophilic residues in the sequence. The length (or size) of the peptide is also a factor in the translocation. In the previously mentioned study by Liao et al., although melittin is the most hydrophobic peptide in the study, it only has the second least energy requirement for translocation because of its relatively large size. The 14-mer peptide LDKA, which happens to be the shortest among the four peptides, also has the smallest energy barrier for crossing (Liao et al., 2023).

Local instability within the membrane leading to deformation can produce transient pore structures. Peptides may take advantage of this in their insertion or translocation mechanism. The formation of small transient micropores in the phosphate region of the pure Re LPS bilayer allowed the entrance of the hydrophobic groups of PmB to enter the core of the model membrane (Jefferies et al., 2017).

***Enhanced Sampling Techniques*.** Enhanced sampling techniques are commonly used to accelerate dynamic processes that are not easily accessible in practical simulation timescales. The problem with equilibrium MD simulations is that it follows the Boltzmann distribution of states visited by a particular system. The configurations that provide the lowest amount of energy will be sampled more frequently, while those that require a high amount of energy will be unlikely. Physical processes requiring energy greater than random thermal fluctuations are considered rare events. In the context of AMP-membrane simulations, peptides with a low propensity to translocate a membrane due to their unfavorable interactions with the membrane are less likely to be seen penetrating a lipid bilayer in a limited simulation time. Since AMPs are usually charged or contain polar residues, their translocation is a rare event and might need enhanced sampling techniques, such as steered MD, to observe the event.

***Steered Molecular Dynamics*.** Steered MD is the process of introducing an imaginary particle that moves at a constant velocity and pulls a chosen molecule, such as the peptide, via the harmonic spring model (Grubmüller et al., 1996). When pulling a peptide into the bilayer, it is vital to consider the collective variable (CV) from which the peptide will be pulled. When extended peptides along the membrane normal are pulled into the bilayer, it will produce less force resistance when the peptide is pulled from the terminal atom close to the membrane compared to pulling it from its center of mass (Likhachev et al., 2022). The latter will allow the peptide to relax and become compact, producing a larger area of resistance. This method will only be helpful when comparing AMPs of similar length to determine how the differences in residue composition affect the energetics of AMP translocation. When comparing peptides with a significantly different number of residues, the greater area of resistance might come from the extra residues in the longer peptide, an unwanted artifact of the simulation design.

***Umbrella Sampling*.** Umbrella sampling is the most common technique to understand membrane-active peptides' permeability across a biological membrane. Here, a starting configuration is defined; in this case, a peptide may be placed some distance above the membrane surface. Usually, the distance is not too large that it will take a long time for the peptide to approach the membrane, but not too short to avoid biasing the initial interaction between the peptide and the membrane. A CV will be defined, and a biasing force will be applied along the CV, forcing the peptide to cross the membrane. Commonly, the CV chosen is the distance along the membrane normal between the center of mass of the peptide and some regions of the membrane model. For example, the average position of the terminal tail beads of the phospholipids in the membrane inner leaflet can be chosen as the zero coordinate. As the center of mass of the peptide moves towards the phosphates of the outer leaflet phospholipids, the coordinate goes in the positive direction. Conversely, as the center of mass of the peptide moves towards the phosphates of the inner leaflet phospholipids, the coordinate goes in the negative direction.

The biased simulation will be run until the peptide has traveled the desired distance or the desired ending configuration is achieved. From the output trajectory, snapshots will be carefully selected and extracted from the original trajectory. Each snapshot will then become the initial configuration for another simulation, but this time, the CV will be restrained such that the peptide will only be allowed to explore the CV space close to it. In choosing the snapshots, one can initially arbitrarily define several systems to run and divide the CV space equally according to this number, including the starting and ending configuration. However, after running the simulations, the CV space explored by each system must be checked. A good umbrella sampling must have each system explore the CV space that will overlap that of its neighbor.

US can be used in calculating the potential of mean force of a peptide as it translocates a biological membrane. This will give us an idea of how much energy the peptide needs to cross the membrane. For example, the energetics insertion of GF-17 AMP, a human cathelicidin LL-37 fragment across DPPG and DPPE/DPPG bilayers, was calculated using umbrella sampling. The majority of the residues in the peptide are hydrophobic, which explains the favorable penetration of the peptide towards the center of the bilayer. The greater proportion of negatively charged lipids in the pure DPPG bilayer led to a greater reduction in free energy of translocation of the peptide in this bilayer (Aghazadeh et al., 2020).

Since the energetics of peptide translocation depends on the nature of amino acids in the AMP and the lipid composition of the bilayer, the peptide can also encounter an energetic barrier as it translocates. Using the US, the PMF profile of translocating PmB across a pure Re LPS bilayer loaded with Na^+ or Ca^{2+} ions was generated (Jefferies et al., 2017). The energy minima were located about 1.6 to 1.9 nm away from the bilayer center where PmB interacts with the negatively charged groups of Re LPS. This agrees with what was observed in unbiased simulations of PmB-Re LPS systems. The interaction free energy of PmB with Re LPS headgroups is about -84 kcal/mol and -130 kcal/mol in the presence of Na^+ and Ca^{2+} ions, respectively (Jefferies et al., 2017). Further decomposition of the energy components confirmed that the negative free energy is enthalpy-driven. The entropy change of the binding process is positive, which they assessed to be contributed by the decrease in configurational entropy of the peptide upon insertion and changes in membrane entropy.

In assessing the crossing of PmB across a more complex model membrane, the energy requirement of inserting PmB across a bacterial membrane was evaluated by doing the US on three different membrane models of different compositions: asymmetric outer membrane (a-OM), LPS-deficient outer membrane, and inner membrane (IM) (Fu et al., 2022). The binding of the peptide on the surface of the lipopolysaccharide (LPS) layer of the a-OM was found to be favorable (-20 kcal/mol), but going further into the membrane requires 70 kcal/mol of energy. The a-OM, in this case, also contains Ca^{2+} as counterions and uses the same MARTINI force field, similar to the earlier discussion. However, the huge discrepancy in the calculated free energy of binding to the LPS (-130 vs. -20) may be due to the difference in lipid composition. The previous study used a symmetric Re LPS bilayer, which may have different entropy changes when PmB binds to the membrane. Interestingly, the binding affinity of an additional peptide to the LPS decreases, but the overall energy requirement for translocation decreases (Fu et al., 2022). A lower amount of energy is needed for the peptide to translocate the IM due to less packing of phospholipids in the IM than the LPS in the a-OM. To make the outer membranes deficient in LPS, the ratio of LPS to phospholipids is decreased. Comparing the translocation of peptides across the pure LPS layer against that of a mixture of LPS and phospholipids, the peptide has the lower energy required to cross the membrane with phospholipids (Fu et al., 2022). The addition of phospholipids allowed for membrane defects, which caused the membrane to become softer and more compressible. Such defects will enable the peptide to penetrate the membrane more easily.

***MD Simulations at Elevated Temperatures*.** It has been demonstrated that transmembrane helical peptides require about 5 kJ mol^{-1} of energy for the hydrogen bonds to be broken

(Ulmschneider et al., In Silico, 2011; Ulmschneider et al., Mechanism, 2010; Ulmschneider et al., Spontaneous, 2014). Translating to k_BT, it means that the transmembrane peptides can remain helical under temperatures as high as 2500 K. This allows such peptides to be studied at relatively high temperatures. This implies that we can accelerate high-energy processes such as pore formation or even test the stability of such pores for as long as the membrane remains stable. Various pore architectures of the AMP maculatin were characterized when the surface-bound peptides were run at temperatures ranging from 80 to 120°C. Pore lifetimes at room temperature were determined by quantifying the pore lifetimes at elevated temperatures and extrapolating to room temperature using the Arrhenius kinetic model (Wang et al., Spontaneous, 2016). Another mechanism of peptide translocation was seen by running simulations at elevated temperatures, wherein the AMP PGLa translocates individually. Here, a few peptides are connected at their termini, forming water bridges and facilitating the movement of charged molecules and water across the membrane (Ulmschneider, 2017).

Running simulations at higher temperatures has provided mechanistic insights into translocation and defect formation. Experimental pores formed by alamethicin peptides were confirmed in an MD study simulated at a high temperature of 140°C and in an external electric field. Initially, surface-bound alamethicins were inserted into the bilayer upon application of the electric field, and the pores were only stable at high temperatures. The electric field is more important in facilitating the insertion, but a high temperature is required for insertion to happen at shorter time scales (Perrin and Pastor, 2016). On the other hand, the AMP piscidin 1, studied by the same group, did not show spontaneous insertion of the peptide under the same conditions. However, when the simulations were initiated from an existing pore assembly of the peptides, the pore was more stable at 40°C and 140°C than at room temperature (Perrin et al., 2016). The differences in these observations were accounted for by the greater number of hydrophobic residues in alamethicin, providing more favorable interactions with the hydrophobic core of the bilayer. The system must be observed carefully when running peptide-membrane simulations at increased temperatures. The high temperature can lead to membrane thinning and increased surface area, distorting the results (Venable et al., 2019).

FORMATION OF AGGREGATED STRUCTURES AND MEMBRANE PORES

Due to the amphiphilic nature of membrane-active peptides, they prefer to be inserted into the membrane as an aggregate rather than a single peptide. Recent literature on peptide-membrane simulations has started to explore the effects of peptide-to-lipid ratio on the insertion dynamics of the peptides (Liao et al., 2023; Sun et al., Organization, 2022). The exposure of hydrophilic residues to the predominantly hydrophobic core of the lipid bilayer requires considerable energy. The insertion mechanisms of AMPs observed over the past few decades, i.e., pore formation and carpet mechanism (Figure 1), require multiple peptides to be inserted into the membrane.

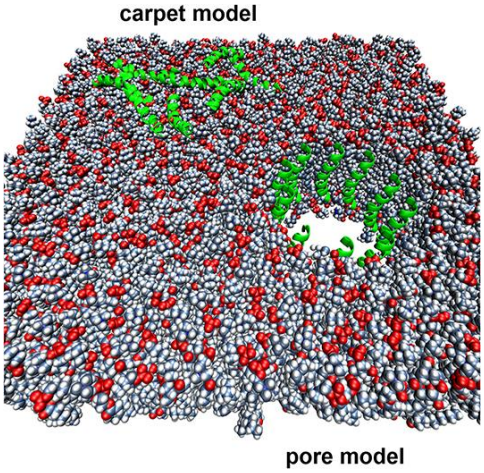

Figure 1. Proposed mechanisms of insertion of antimicrobial peptides into a lipid bilayer. Red spheres are the lipid headgroups, gray spheres are the lipid acyl chains, and green ribbon structures are the antimicrobial peptides. Reproduced with permission from (Mercer et al., 2020).

Suppose peptide aggregation is significant when inserted into the membrane. In that case, it is therefore essential to consider the interaction between peptides during peptide design, in addition to the interaction of the peptide with the hydrophilic and hydrophobic regions of the membrane. The biomimetic 14-mer peptide LDKA cannot cross the membrane alone, thus requiring the formation of an aggregated structure before it can further penetrate the hydrophilic region of the bilayer (Chen et al., 2019). The LDKA oligomers formed upon binding to a DPPG bilayer become a cluster from dimer as the number of LDKA monomers increases. Once aggregated, stable nanopores form at a critical peptide-to-lipid ratio that varies from one peptide to another (Liao et al., 2023). This agrees with the modified carpet model proposed by Rathinakumar et al. (Rathinakumar and Wimley, 2008), where self-assembly occurs at the bilayer surface at the beginning of membrane disruption. As suggested by both experimental and MD studies, the scaffold nanostructures that form pores comprise peptides, lipids, water, and ions. Melittin was also seen to aggregate into nanostructures and form a thick layer below the DPPG bilayer. This layer prevents membrane disruption, which is evident from a more visible membrane disruption at an aggregate with fewer melittin monomers (Liao et al., 2023). Longer coarse-grained simulations of multiple melittins interacting with DPPC/POPG lipid bilayer showed different sets of aggregate structures, where the peptides are either transmembrane (T-peptide) or U-shaped (U-peptide) (Sun et al., Organization, 2022). The ends of the T-peptide are at the two different leaflets of the membrane. On the other hand, the ends of the U-peptide are at the same membrane leaflet. The T-peptides have more negative binding energy when aggregating with other peptides than a single transmembrane peptide (Sun et al., Organization, 2022). The AMP polymyxin B (PMB) was also seen to aggregate on the surface of an outer membrane model containing LPS (Berglund et al., 2015). The peptides bury their hydrophobic tails, creating a micelle-like conformation (Figure 2). This is the hydrophobic effect brought by the wide presence of sugar rings in the LPS molecules.

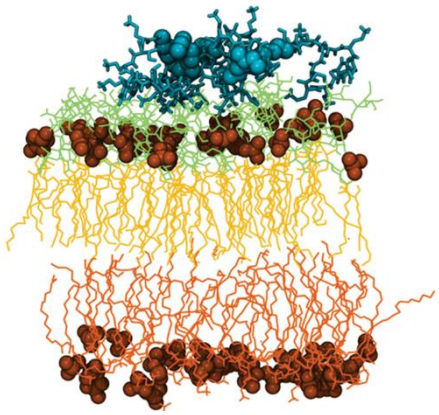

Figure 2. Aggregation of melittin peptides in a micelle-like conformation, with hydrophobic tails buried in the core of the aggregate. Legend: PMB1 non-tail: cyan, licorice format; PMB1 tail: cyan, VdW format; lipid phosphate groups: orange, VdW format; LPS sugars: lime, lines format; LPS phospholipids: orange, lines format. Reproduced with permission from (Berglund et al., 2015).

Another observed mechanism (Figure 3) involving peptide aggregation showed the initial induction of membrane curvature by a single melittin peptide. This is followed by an aggregation of four melittin peptides to penetrate the bilayer cooperatively. A toroidal pore opened as the peptides were inserted deeper into the membrane (Miyazaki and Shinoda, 2022). The radius of the pore formed was evaluated using the HOLE program (Smart et al., 1996), and the value agreed with the experimental results.

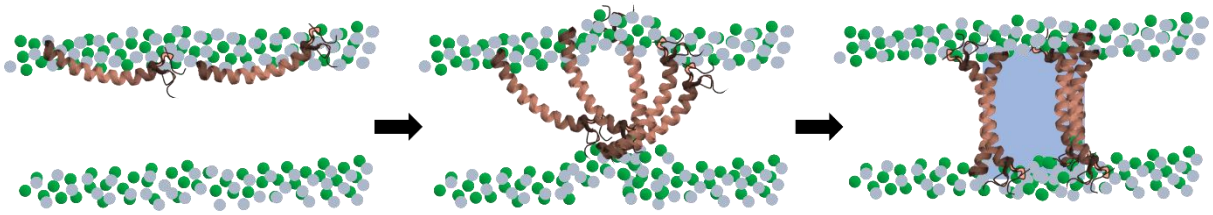

Figure 3. Toroidal pore formation mechanism of melittin peptides initiated from a membrane curvature followed by aggregation.

The formation of pores may be monitored by determining the number of water molecules present in the hydrophobic core of the bilayer. For example, the presence of pores in a 70:30 PC:PG bilayer due to aggregation of melittin was detected by calculating the number of water molecules in the 1 nm slab around the bilayer center (Figure 4) (Santo et al., 2013). The sharp increase in water molecules at around 3560 ns and 12500 ns suggested the formation of a transient water pore. In addition, a time-averaged water density plot can also be calculated to detect water defects (Figure 5) (Santo et al., 2013). This is a three-dimensional plot where one axis represents the x-axis of the system and the second axis represents the membrane normal axis. The third dimension is a color scheme that shows the fraction of water molecules for every xz position. This can identify water defects from pore formation due to melittin aggregation. The water defects in a bilayer without the peptides are also generated for comparison.

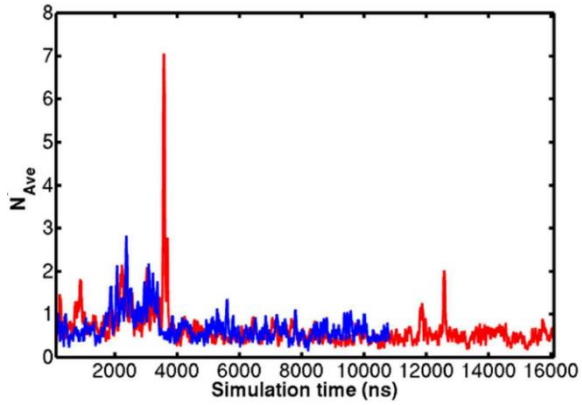

Figure 4. Running average of water molecules (N_{Ave}) within 1 nm of the bilayer center for two different simulation replicates of melittin in PC:PG bilayer. Reprinted with permission from (Santo et al., 2013). Copyright 2013 American Chemical Society.

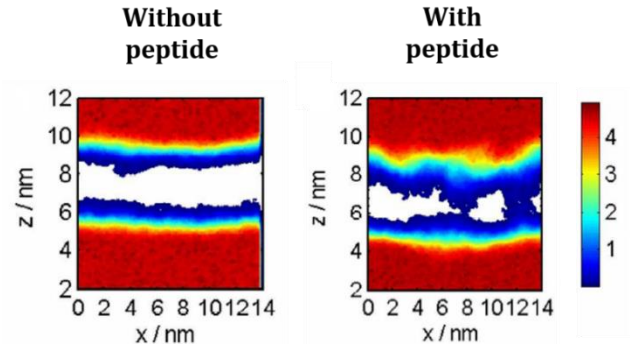

Figure 5. Frequency of water molecules in the xz plane of a PC:PG bilayer. The left panel shows the average water defects in the absence of melittin peptides. The right panel shows the average water defects in the presence of melittin peptides. Reprinted with permission from (Santo et al., 2013). Copyright 2013 American Chemical Society.

EFFECT OF PEPTIDES ON MEMBRANE PROPERTIES

In maintaining the structure and integrity of the cell membrane, lipid transferases, and flippases all function to keep lipid homeostasis. As AMPs are foreign to cells, they have enormous potential to alter different membrane properties, which may lead to membrane disruption. The common membrane properties measured are area per lipid and membrane thickness.

Membrane Thickness. For a homogeneous lipid bilayer, membrane thickness can be determined by choosing a set of atoms from the headgroup of the lipids, usually phosphates, getting the time and ensemble-average center-of-mass (COM) along the membrane normal of this set in each leaflet, and calculating the absolute difference of these average COMs (Berglund et al., 2015). Some MD simulations create a density profile of the phosphates from the phospholipids along the membrane normal and define the peak-to-peak separation as the membrane thickness (Li et al., 2013). A membrane analysis tool called APL@Voro (Kern et al., 2023; Lukat et al., 2013) is available to more accurately calculate the membrane thickness, especially for heterogeneous lipid bilayers that can have biphasic nature (Fu et al., 2022).

Area per Lipid. Regardless of the lipid composition of the bilayer, the instantaneous area per lipid is calculated as the area of the x-y plane divided by the number of lipids in any leaflets. For asymmetric bilayers, it is essential to note that the area per lipid will be different for the two leaflets. Using the ensemble-average area per lipid, $\langle A_L \rangle$, the isothermal area compressibility modulus, K_A, of the bilayer can be calculated by:

$$K_A = \frac{2k_B\langle T\rangle\langle A_L\rangle}{N_L\sigma^2} \qquad \text{Equation 1}$$

where k_B is the Boltzmann constant, $\langle T\rangle$ is the ensemble-average temperature, N_L is the number of lipids in one leaflet, and σ^2 is the variance of A_L. This compressibility modulus can be thought of as a spring constant for lateral compression or stretching of the bilayer (Nagle, 2019). A higher modulus would mean the bilayer is more difficult to compress laterally. This is also associated with the energetic cost of stretching or compressing the area (Doktorova et al., 2019). Due to the undulations in modeling realistic biological membranes, the true area per lipid must be calculated differently. For better area per lipid calculations, we can look at a review paper that summarizes available tools for analyzing general membrane properties (Guo et al., 2023).

Generally, there is an observed increase in area per lipid and membrane thinning upon the interaction of AMPs with model membranes. Polymyxin B, for example, causes the release of calcium ions initially bound to the membrane, resulting in the loosening of LPS packing and increasing membrane area. It also deforms the asymmetric stress profiles of a Gram-negative bacterial outer membrane model by shifting stress toward the inner leaflet (Fu et al., 2022). Nanoaggregates of G4 peptides ($G(IIKK)_4I\text{-}NH_2$) were able to reduce the bilayer thickness by pulling the lipid head groups toward the center of the bilayer via interaction with the hydrophilic outer surface of the G4 aggregates (Liao et al., 2023). In the simulation of GF-17 with DPPG and DPPE/DPPG bilayers, an increase in area per lipid was likewise observed, but there were no significant changes in membrane thickness (Aghazadeh et al., 2020). Membrane thinning and an increase in area per lipid were also observed in the interaction of Clavanin A with a POPE/POPG model membrane (Duay et al., 2019). Divalent cations, commonly used by organisms, such as Ca^{2+} and Zn^{2+}, have opposite effects on these membrane properties to a certain extent (Kučerka et al., 2017). Interestingly, it seems that there is a critical membrane thickness that must be achieved for an AMP to penetrate spontaneously. The thinning caused by melittin peptides led to penetration once the membrane thickness leveled off (Sun et al., Organization, 2022).

Membrane Phases. Analyzing the area per lipid distribution of the membrane can reveal different phases in the membrane. In a study by Jefferies et al., the non-Gaussian distribution of the area per lipid of a symmetric Re LPS bilayer suggested that there are regions of the membrane that are tightly packed and domains that are loosely packed (Jefferies et al., 2017). They also presented a peculiar method of characterizing the phases better by calculating the wavenumber-dependent viscosity using transverse current autocorrelation functions. The static viscosity of the membrane model is only about three to four times greater than that of water, indicating fluidity. However, when the same calculations were applied to the phosphate groups only, the viscosity was calculated to be at least 1000 times greater than the rest of the membrane model, comparable to the viscosities of molten glass (Jefferies et al., 2017). This suggests that the Re LPS bilayer has both fluid-like and glass-like properties but in different membrane regions. In the presence of PmB, small, ordered domains are induced, and crystal patches of Re LPS headgroups are formed.

Density Distribution of Lipid Bilayer Regions. Another way to characterize the lipid bilayer is by calculating the mass density distribution of specific regions in the lipid bilayer concerning its distance from the bilayer center along the membrane normal. This helps compare any significant movements in the membrane as the peptide interacts with it. Furthermore, this will locate the region where the peptide stays in most parts of the simulation. The effect of binding the AMPs myxinidin and WMR, for example, revealed membrane thinning and the introduction of asymmetry to the lipid distribution between the two leaflets (Cherniavskyi et al., 2024). The membrane thinning can be interpreted from the movement of the density peaks of the different membrane components closer to the center in the presence of the peptides, as compared against the negative control with the bilayer only.

Line Tension. When domains form within the membrane or lipids undergo phase separation, there is an interfacial energy at the edge of these domains or phases called line tension. This can also be seen as the energy required per unit length to build the interface between membrane domains. The equation used to calculate line tension is (Miyazaki et al., 2019):

$$\Lambda = \frac{1}{2}\langle L_x L_z \left[\frac{1}{2}(P_{xx} + P_{zz}) - P_{yy}\right]\rangle \qquad \text{Equation 2}$$

where L_x and L_z are cell lengths along x and z, respectively, and P_{xx}, P_{yy}, and P_{zz} are the pressure along the x, y, and z axes, respectively. In determining the effect of melittin on the line tension of a purely PC membrane, a membrane with ribbon-like geometry was set up by having a fixed cell length along the ribbon axis (y-axis). The line tension at the bilayer edge will induce a tendency to minimize the length along the y-axis. The pressure along the y-axis was monitored, while the x- and z-axis pressure was fixed at 1 bar with isotropic coupling. Their results showed that melittin decreases the line tension significantly in an amount-dependent manner, suggesting that melittin is a pore-forming peptide.

CONCLUSIONS AND FUTURE PERSPECTIVES

One of the significant challenges in simulating systems with lipid bilayer is equilibration. When looking at the peptide interaction with a lipid bilayer in an MD simulation, it is essential to equilibrate the model membrane before introducing the peptide. Otherwise, the initial conditions, e.g., aggregation of one type of lipid in a particular region, may bias the simulation results. However, for lipid bilayers with heterogeneous composition, the equilibration may require an unreasonable amount of physical time (Sodt et al., 2014). Most, if not all, simulations will run hundreds (Liao et al., 2023) to thousands (Fu et al., 2022) of nanoseconds of the solvated lipid bilayer (without the peptide) and report that the bilayer is already equilibrated without showing any temporal-converged bilayer parameter.

The parameters that may be monitored for equilibration are area per lipid, membrane thickness, and lipid lateral diffusion coefficient. In investigating the effect of peptides on heterogeneous lipid bilayers, it might be necessary that the lateral diffusion coefficient is allowed to converge first before initiating any interaction between the peptide and the membrane. This allows for the mixing of the different lipid types in the bilayer (Wang et al., Enhanced, 2011). Not doing so may lead to an incorrect interpretation of the peptide influencing the lipid diffusion coefficient when it is just an artifact of the bilayer undergoing equilibration. Accelerated molecular dynamics is a technique that can be done to equilibrate a model membrane in accessible shorter time scales (Wang et al., Enhanced, 2011).

An aspect of the simulation systems that must be considered carefully is the lipid composition of the model membrane. For antimicrobial peptides to be effective, they must interact well with the cell membrane of their target while avoiding communicating with the cell membrane of the host cells. The difference in lipid composition between bacterial and human cell membranes will affect the antimicrobial activity of an AMP (Matsuzaki, 1999; Zasloff, 2002). Therefore, an aspect that must be carefully considered in running MD simulations of AMPs with lipid bilayers is the composition of the model membrane. In an earlier section, more realistic model membranes are more complex, but they provide additional mechanistic insights, especially if the model is atomistic. The length of the lipid tail also influences the dynamics of the AMP, as the membrane thickness depends on this (Song et al., 2019).

Finally, a membrane property that has yet to be considered in any MD simulations involving AMPs is the membrane curvature. Each mechanism of action of AMPs provides its distinct cytological profile, including the membrane circularity (Juliano et al., 2020). This now begs the question: Do

these AMPs induce these changes in the membrane curvature? A previous article by Schmidt and Wong (Schmidt and Wong, 2013) shed some light on this question, stating that both AMPs and lipid composition play a role in the induction of membrane curvature. It seems that stronger electrostatic interactions will result in greater curvature deformation. Another mechanistic question may be whether AMPs have preferential interaction with curved membranes over relatively flat membranes. As there are now tools that can be used to model curved membranes (Boyd and May, 2018; Yesylevskyy and Khandelia, 2021), and MD simulations on curved membranes are already being done over recent years (Larsen, 2022; Yesylevskyy and Ramseyer, 2014), it is about time for the field to start on looking at how we can introduce AMPs to pre-existing curved membranes.

As high-performance computing technology moves forward, the extent to which we can investigate these mechanisms becomes larger. Greater computational power means running millisecond-long simulations may eventually be done in routine MD work. A sampling of peptide translocation may be enhanced without needing to bias the system. Overall, the use of MD simulations in understanding the mechanism of action of different antimicrobial peptides as they interact with different model membranes looks promising.

REFERENCES

Aghazadeh H, Ganjali Koli M, Ranjbar R, Pooshang Bagheri K. Interactions of GF-17 derived from LL-37 antimicrobial peptide with bacterial membranes: a molecular dynamics simulation study. J Computer-Aided Molecular Design. 2020 Dec; 34(12):1261–1273. https://doi.org/10.1007/s10822-020-00348-4

Andreu D, Ubach J, Boman A, Wåhlin B, Wade D, Merrifield RB, et al. Shortened cecropin A-melittin hybrids Significant size reduction retains potent antibiotic activity. FEBS Letters. 1992 Jan; 296(2):190–194. https://doi.org/10.1016/0014-5793(92)80377-S

Balandin SV, Ovchinnikova TV. Antimicrobial peptides of invertebrates. Part 2. biological functions and mechanisms of action. Russian J Bioorg Chem. 2016 Jul; 42(4):343–360. https://doi.org/10.1134/S106816201604004X

Barrera EE, Machado MR, Pantano S. Fat SIRAH: Coarse-Grained Phospholipids To Explore Membrane–Protein Dynamics. J Chem Theory Comput 2019 Oct; 15(10):5674–5688. https://doi.org/10.1021/acs.jctc.9b00435

Bennett WFD, Hong CK, Wang Y, Tieleman DP. Antimicrobial Peptide Simulations and the Influence of Force Field on the Free Energy for Pore Formation in Lipid Bilayers. J Chem Theory Comput. 2016 Sep; 12(9):4524–4533. https://doi.org/10.1021/acs.jctc.6b00265

Berglund NA, Piggot TJ, Jefferies D, Sessions RB, Bond PJ, Khalid S. Interaction of the antimicrobial peptide polymyxin B1 with both membranes of E. coli: a molecular dynamics study. PLoS Comput Biol. 2015 Apr; 11(4):e1004180. https://doi.org/10.1371/journal.pcbi.1004180

Best RB, Zhu X, Shim J, Lopes PEM, Mittal J, Feig M, et al. Optimization of the Additive CHARMM All-Atom Protein Force Field Targeting Improved Sampling of the Backbone ϕ, ψ and Side-Chain χ1 and χ2 Dihedral Angles. J Chem Theory Comput. 2012 Sep; 8(9):3257–3273. https://doi.org/10.1021/ct300400x

Bhattacharjya S, Straus SK. Design, Engineering and Discovery of Novel α-Helical and β-Boomerang Antimicrobial Peptides against Drug Resistant Bacteria. Int J Molec Sci. 2020; 21(16)https://doi.org/10.3390/ijms21165773

Boyd KJ, May ER. BUMPy: A Model-Independent Tool for Constructing Lipid Bilayers of Varying Curvature and Composition. J Chem Theory Comput. 2018 Dec; 14(12):6642–6652. https://doi.org/10.1021/acs.jctc.8b00765

Chen CH, Starr CG, Troendle E, Wiedman G, Wimley WC, Ulmschneider JP, et al. Simulation-Guided Rational de Novo Design of a Small Pore-Forming Antimicrobial Peptide. J Am Chem Soc. 2019 Mar; 141(12):4839–4848. https://doi.org/10.1021/jacs.8b11939

Cherniavskyi YK, Oliva R, Stellato M, Del Vecchio P, Galdiero S, Falanga A, et al. Structural characterization of the antimicrobial peptides myxinidin and WMR in bacterial membrane mimetic micelles and bicelles. Biochimica et Biophysica Acta (BBA) - Biomembranes. 2024 Mar; 1866(3):184272. https://doi.org/10.1016/j.bbamem.2024.184272

Clausell A, Garcia-Subirats M, Pujol M, Busquets MA, Rabanal F, Cajal Y. Gram-Negative Outer and Inner Membrane Models: Insertion of Cyclic Cationic Lipopeptides. J Phys Chem B. 2007 Jan; 111(3):551–563. https://doi.org/10.1021/jp064757+

Cockcroft S. Mammalian lipids: structure, synthesis and function. Essays Biochem. 2021 Nov; 65(5):813–845. https://doi.org/10.1042/EBC20200067

Conklin SE, Bridgman EC, Su Q, Riggs-Gelasco P, Haas KL, Franz KJ. Specific Histidine Residues Confer Histatin Peptides with Copper-Dependent Activity against Candida albicans. Biochem. 2017 Aug; 56(32):4244–4255. https://doi.org/10.1021/acs.biochem.7b00348

Doktorova M, LeVine MV, Khelashvili G, Weinstein H. A New Computational Method for Membrane Compressibility: Bilayer Mechanical Thickness Revisited. Biophysical J. 2019 Feb; 116(3):487–502. https://doi.org/10.1016/j.bpj.2018.12.016

Duay SS, Sharma G, Prabhakar R, Angeles-Boza AM, May ER. Molecular Dynamics Investigation into the Effect of Zinc(II) on the Structure and Membrane Interactions of the Antimicrobial Peptide Clavanin A. J Phys Chem B. 2019 Apr; 123(15):3163–3176. https://doi.org/10.1021/acs.jpcb.8b11496

Duong F, Eichler J, Price A, Rice Leonard M, Wickner W. Biogenesis of the Gram-Negative Bacterial Envelope. Cell. 1997 Nov; 91(5):567–573. https://doi.org/10.1016/S0092-8674(00)80444-4

Ehrenstein G, Lecar H. Electrically gated ionic channels in lipid bilayers. Q Rev Biophys. 1977 Feb; 10(1):1–34. https://doi.org/10.1017/s0033583500000123

Fadda E, Woods RJ. Molecular simulations of carbohydrates and protein-carbohydrate interactions: motivation, issues and prospects. Drug Discov Today. 2010 Aug; 15(15–16):596–609. https://doi.org/10.1016/j.drudis.2010.06.001

Feller SE, Yin D, Pastor RW, MacKerell AD. Molecular dynamics simulation of unsaturated lipid bilayers at low hydration: parameterization and comparison with diffraction studies. Biophysical J. 1997 Nov; 73(5):2269–2279. https://doi.org/10.1016/S0006-3495(97)78259-6

Fjell CD, Hiss JA, Hancock REW, Schneider G. Designing antimicrobial peptides: form follows function. Nature Reviews Drug Discov. 2012 Jan; 11(1):37–51. https://doi.org/10.1038/nrd3591

Fu L, Li X, Zhang S, Dong Y, Fang W, Gao L. Polymyxins induce lipid scrambling and disrupt the homeostasis of Gram-negative bacteria membrane. Biophysical J. 2022 Sep; 121(18):3486–3498. https://doi.org/10.1016/j.bpj.2022.08.007

Fu L, Wan M, Zhang S, Gao L, Fang W. Polymyxin B Loosens Lipopolysaccharide Bilayer but Stiffens Phospholipid Bilayer. Biophysical J. 2020 Jan; 118(1):138–150. https://doi.org/10.1016/j.bpj.2019.11.008

Gharaghani S, Khayamian T, Ebrahimi M. Molecular dynamics simulation study and molecular docking descriptors in structure-based QSAR on acetylcholinesterase (AChE) inhibitors. SAR QSAR Environ Res. 2013; 24(9):773–794. https://doi.org/10.1080/1062936X.2013.792877

Ghosh D, Porter E, Shen B, Lee SK, Wilk D, Drazba J, et al. Paneth cell trypsin is the processing enzyme for human defensin-5. Nature Immunology. 2002 Jun; 3(6):583–590. https://doi.org/10.1038/ni797

Grubmüller H, Heymann B, Tavan P. Ligand Binding: Molecular Mechanics Calculation of the Streptavidin-Biotin Rupture Force. Science. 1996 Feb; 271(5251):997–999. https://doi.org/10.1126/science.271.5251.997

Guo J, Bao Y, Li M, Li S, Xi L, Xin P, et al. Application of computational approaches in biomembranes: From structure to function. WIREs Comput Molec Sci. 2023 Nov; 13(6):e1679. https://doi.org/10.1002/wcms.1679

Hénin J, Lelièvre T, Shirts MR, Valsson O, Delemotte L. Enhanced Sampling Methods for Molecular Dynamics Simulations [Article v1.0]. Living J Comp Mol Sci. 2022 Dec; 4(1):1583. https://doi.org/10.33011/livecoms.4.1.1583

Huang J, Rauscher S, Nawrocki G, Ran T, Feig M, de Groot BL, et al. CHARMM36m: an improved force field for folded and intrinsically disordered proteins. Nat Methods. 2017 Jan; 14(1):71–73. https://doi.org/10.1038/nmeth.4067

Irudayam SJ, Berkowitz ML. Binding and reorientation of melittin in a POPC bilayer: Computer simulations. Biochimica et Biophysica Acta (BBA) - Biomembranes. 2012 Dec; 1818(12):2975–2981. https://doi.org/10.1016/j.bbamem.2012.07.026

Jefferies D, Hsu PC, Khalid S. Through the Lipopolysaccharide Glass: A Potent Antimicrobial Peptide Induces Phase Changes in Membranes. Biochem. 2017 Mar; 56(11):1672–1679. https://doi.org/10.1021/acs.biochem.6b01063

Juliano SA, Pierce S, deMayo JA, Balunas MJ, Angeles-Boza AM. Exploration of the Innate Immune System of Styela clava: Zn2+ Binding Enhances the Antimicrobial Activity of the Tunicate Peptide Clavanin A. Biochem. 2017 Mar; 56(10):1403–1414. https://doi.org/10.1021/acs.biochem.6b01046

Juliano SA, Serafim LF, Duay SS, Heredia Chavez M, Sharma G, Rooney M, et al. A Potent Host Defense Peptide Triggers DNA Damage and Is Active against Multidrug-Resistant Gram-Negative Pathogens. ACS Infect Dis. 2020 May; 6(5):1250–1263. https://doi.org/10.1021/acsinfecdis.0c00051

Kern M, Jaeger-Honz S, Schreiber F, Sommer B. APL@voro—interactive visualization and analysis of cell membrane simulations. Bioinformatics. 2023 Feb; 39(2):btad083. https://doi.org/10.1093/bioinformatics/btad083

Klauda JB, Venable RM, Freites JA, O'Connor JW, Tobias DJ, Mondragon-Ramirez C, et al. Update of the CHARMM All-Atom Additive Force Field for Lipids: Validation on Six Lipid Types. J Phys Chem B. 2010 Jun; 114(23):7830–7843. https://doi.org/10.1021/jp101759q

Koike M, Iida K, Matsuo T. Electron microscopic studies on mode of action of polymyxin. J Bacteriol. 1969 Jan; 97(1):448–452. https://doi.org/10.1128/jb.97.1.448-452.1969

Kučerka N, Dushanov E, Kholmurodov KT, Katsaras J, Uhríková D. Calcium and Zinc Differentially Affect the Structure of Lipid Membranes. Langmuir. 2017 Mar; 33(12):3134–3141. https://doi.org/10.1021/acs.langmuir.6b03228

Lai Y, Gallo RL. AMPed up immunity: how antimicrobial peptides have multiple roles in immune defense. Trends Immunol. 2009 Mar; 30(3):131–141. https://doi.org/10.1016/j.it.2008.12.003

Larsen AH. Molecular Dynamics Simulations of Curved Lipid Membranes. Int J Molec Sci. 2022; 23(15). https://doi.org/10.3390/ijms23158098

Lee J, Cheng X, Swails JM, Yeom MS, Eastman PK, Lemkul JA, et al. CHARMM-GUI Input Generator for NAMD, GROMACS, AMBER, OpenMM, and CHARMM/OpenMM Simulations Using the CHARMM36 Additive Force Field. J Chem Theory Comput. 2016 Jan; 12(1):405–413. https://doi.org/10.1021/acs.jctc.5b00935

Lee TH, Hall KN, Aguilar MI. Antimicrobial Peptide Structure and Mechanism of Action: A Focus on the Role of Membrane Structure. Curr Top Med Chem. 2016; 16(1):25–39. https://doi.org/10.2174/1568026615666150703121700

Li J, Liu S, Lakshminarayanan R, Bai Y, Pervushin K, Verma C, et al. Molecular simulations suggest how a branched antimicrobial peptide perturbs a bacterial membrane and enhances permeability. Biochimica et Biophysica Acta (BBA) - Biomembranes. 2013 Mar; 1828(3):1112–1121. https://doi.org/10.1016/j.bbamem.2012.12.015

Liao M, Gong H, Quan X, Wang Z, Hu X, Chen Z, et al. Intramembrane Nanoaggregates of Antimicrobial Peptides Play a Vital Role in Bacterial Killing. Small. 2023 Jan; 19(3):e2204428. https://doi.org/10.1002/smll.202204428

Libardo MDJ, Bahar AA, Ma B, Fu R, McCormick LE, Zhao J, et al. Nuclease activity gives an edge to host-defense peptide piscidin 3 over piscidin 1, rendering it more effective against persisters and biofilms. FEBS J. 2017 Nov; 284(21):3662–3683. https://doi.org/10.1111/febs.14263

Likhachev IV, Balabaev NK, Galzitskaya OV. Is It Possible to Find an Antimicrobial Peptide That Passes the Membrane Bilayer with Minimal Force Resistance? An Attempt at a Predictive Approach by Molecular Dynamics Simulation. Int J Molec Sci. 2022; 23(11). https://doi.org/10.3390/ijms23115997

Ludtke SJ, He K, Heller WT, Harroun TA, Yang L, Huang HW. Membrane Pores Induced by Magainin. Biochem. 1996 Jan; 35(43):13723–13728. https://doi.org/10.1021/bi9620621

Lukat G, Krüger J, Sommer B. APL@Voro: A Voronoi-Based Membrane Analysis Tool for GROMACS Trajectories. J Chem Inf Model. 2013 Nov; 53(11):2908–2925. https://doi.org/10.1021/ci400172g

MacKerell ADJr, Bashford D, Bellott M, Dunbrack RLJr, Evanseck JD, Field MJ, et al. All-Atom Empirical Potential for Molecular Modeling and Dynamics Studies of Proteins. J Phys Chem B. 1998 Apr; 102(18):3586–3616. https://doi.org/10.1021/jp973084f

Mackerell Jr. AD, Feig M, Brooks III CL. Extending the treatment of backbone energetics in protein force fields: Limitations of gas-phase quantum mechanics in reproducing protein conformational

distributions in molecular dynamics simulations. J Comput Chem. 2004 Aug; 25(11):1400–1415. https://doi.org/10.1002/jcc.20065

Mancheño JM, Oñaderra M, Martínez del Pozo A, Díaz-Achirica P, Andreu D, Rivas L, et al. Release of Lipid Vesicle Contents by an Antibacterial Cecropin A–Melittin Hybrid Peptide. Biochem. 1996 Jan; 35(30):9892–9899. https://doi.org/10.1021/bi953058c

Mares J, Kumaran S, Gobbo M, Zerbe O. Interactions of Lipopolysaccharide and Polymyxin Studied by NMR Spectroscopy*. J Biol Chem. 2009 Apr; 284(17):11498–11506. https://doi.org/10.1074/jbc.M806587200

Marrink SJ, Risselada HJ, Yefimov S, Tieleman DP, de Vries AH. The MARTINI Force Field: Coarse Grained Model for Biomolecular Simulations. J Phys Chem B. 2007 Jul; 111(27):7812–7824. https://doi.org/10.1021/jp071097f

Marrink SJ, de Vries AH, Mark AE. Coarse Grained Model for Semiquantitative Lipid Simulations. J Phys Chem B. 2004 Jan; 108(2):750–760. https://doi.org/10.1021/jp036508g

Matsuzaki K. Why and how are peptide–lipid interactions utilized for self-defense? Magainins and tachyplesins as archetypes. Biochimica et Biophysica Acta (BBA) - Biomembranes. 1999 Dec; 1462(1):1–10. https://doi.org/10.1016/S0005-2736(99)00197-2

Mercer DK, Torres MDT, Duay SS, Lovie E, Simpson L, von Köckritz-Blickwede M, et al. Antimicrobial Susceptibility Testing of Antimicrobial Peptides to Better Predict Efficacy. Frontiers Cellular Infection Microbiol. 2020; 10. https://doi.org/10.3389/fcimb.2020.00326

Miyazaki Y, Okazaki S, Shinoda W. Free energy analysis of membrane pore formation process in the presence of multiple melittin peptides. Biochimica et Biophysica Acta (BBA) - Biomembranes. 2019 Jul; 1861(7):1409–1419. https://doi.org/10.1016/j.bbamem.2019.03.002

Miyazaki Y, Shinoda W. Cooperative antimicrobial action of melittin on lipid membranes: A coarse-grained molecular dynamics study. Biochimica et Biophysica Acta (BBA) - Biomembranes. 2022 Sep; 1864(9):183955. https://doi.org/10.1016/j.bbamem.2022.183955

Nagle JF. Area Compressibility Moduli of the Monolayer Leaflets of Asymmetric Bilayers from Simulations. Biophysical J. 2019 Sep; 117(6):1051–1056. https://doi.org/10.1016/j.bpj.2019.08.016

Orsi M, Essex JW. The ELBA Force Field for Coarse-Grain Modeling of Lipid Membranes. PLOS ONE. 2011 Dec; 6(12):e28637. https://doi.org/10.1371/journal.pone.0028637

Ouyang J, Sheng Y, Wang W. Recent Advances of Studies on Cell-Penetrating Peptides Based on Molecular Dynamics Simulations. Cells. 2022; 11(24). https://doi.org/10.3390/cells11244016

Palmer N, Maasch JRMA, Torres MDT, de la Fuente-Nunez C. Molecular Dynamics for Antimicrobial Peptide Discovery. Infect Immun. 2021 Mar; 89(4). https://doi.org/10.1128/IAI.00703-20

Pan Y, Lu Z, Li C, Qi R, Chang H, Han L, et al. Molecular Dockings and Molecular Dynamics Simulations Reveal the Potency of Different Inhibitors against Xanthine Oxidase. ACS Omega. 2021 May; 6(17):11639–11649. https://doi.org/10.1021/acsomega.1c00968

Perrin BS, Fu R, Cotten ML, Pastor RW. Simulations of Membrane-Disrupting Peptides II: AMP Piscidin 1 Favors Surface Defects over Pores. Biophysical J. 2016 Sep; 111(6):1258–1266. https://doi.org/10.1016/j.bpj.2016.08.015

Perrin BS, Pastor RW. Simulations of Membrane-Disrupting Peptides I: Alamethicin Pore Stability and Spontaneous Insertion. Biophysical J. 2016 Sep; 111(6):1248–1257. https://doi.org/10.1016/j.bpj.2016.08.014

Poger D, Mark AE. Lipid Bilayers: The Effect of Force Field on Ordering and Dynamics. J Chem Theory Comput. 2012 Nov; 8(11):4807–4817. https://doi.org/10.1021/ct300675z

Rajagopal M, Walker S. Envelope Structures of Gram-Positive Bacteria. Curr Top Microbiol Immunol. 2017; 404:1–44. https://doi.org/10.1007/82_2015_5021

Rathinakumar R, Wimley WC. Biomolecular Engineering by Combinatorial Design and High-Throughput Screening: Small, Soluble Peptides That Permeabilize Membranes. J Am Chem Soc. 2008 Jul; 130(30):9849–9858. https://doi.org/10.1021/ja8017863

Rice LB. Federal Funding for the Study of Antimicrobial Resistance in Nosocomial Pathogens: No ESKAPE. J Infect Diseases. 2008 Apr; 197(8):1079–1081. https://doi.org/10.1086/533452

Rice LB. Progress and challenges in implementing the research on ESKAPE pathogens. Infect Control Hosp Epidemiol. 2010 Nov; 31 Suppl 1:S7-10. https://doi.org/10.1086/655995

Sahoo BR, Fujiwara T. Membrane Mediated Antimicrobial and Antitumor Activity of Cathelicidin 6: Structural Insights from Molecular Dynamics Simulation on Multi-Microsecond Scale. PLOS ONE. 2016 Jul; 11(7):e0158702. https://doi.org/10.1371/journal.pone.0158702

Santo KP, Berkowitz ML. Difference between Magainin-2 and Melittin Assemblies in Phosphatidylcholine Bilayers: Results from Coarse-Grained Simulations. J Phys Chem B. 2012 Mar; 116(9):3021–3030. https://doi.org/10.1021/jp212018f

Santo KP, Irudayam SJ, Berkowitz ML. Melittin Creates Transient Pores in a Lipid Bilayer: Results from Computer Simulations. J Phys Chem B. 2013 May; 117(17):5031–5042. https://doi.org/10.1021/jp312328n

Santos DES, Pol-Fachin L, Lins RD, Soares TA. Polymyxin Binding to the Bacterial Outer Membrane Reveals Cation Displacement and Increasing Membrane Curvature in Susceptible but Not in Resistant Lipopolysaccharide Chemotypes. J Chem Inf Model. 2017 Sep; 57(9):2181–2193. https://doi.org/10.1021/acs.jcim.7b00271

Schlenkrich M, Brickmann J, MacKerell AD, Karplus M. An Empirical Potential Energy Function for Phospholipids: Criteria for Parameter Optimization and Applications. InMerz KM, Roux B, editors.Biological Membranes: A Molecular Perspective from Computation and Experiment. Boston, MA: Birkhäuser Boston;1996.p. 31–81. https://doi.org/10.1007/978-1-4684-8580-6_2

Schmidt NW, Wong GCL. Antimicrobial peptides and induced membrane curvature: Geometry, coordination chemistry, and molecular engineering. Current Opinion in Solid State and Materials Science. 2013 Aug; 17(4):151–163. https://doi.org/10.1016/j.cossms.2013.09.004

Sengupta D, Leontiadou H, Mark AE, Marrink SJ. Toroidal pores formed by antimicrobial peptides show significant disorder. Biochimica et Biophysica Acta (BBA) - Biomembranes. 2008 Oct; 1778(10):2308–2317. https://doi.org/10.1016/j.bbamem.2008.06.007

Seo S, Shinoda W. SPICA Force Field for Lipid Membranes: Domain Formation Induced by Cholesterol. J Chem Theory Comput. 2019 Jan; 15(1):762–774. https://doi.org/10.1021/acs.jctc.8b00987

Shai Y. Mechanism of the binding, insertion and destabilization of phospholipid bilayer membranes by α-helical antimicrobial and cell non-selective membrane-lytic peptides. Biochimica et Biophysica Acta (BBA) - Biomembranes. 1999 Dec; 1462(1):55–70. https://doi.org/10.1016/S0005-2736(99)00200-X

Shi N, Zheng Q, Zhang H. Molecular Dynamics Investigations of Binding Mechanism for Triazoles Inhibitors to CYP51. Front Molec Biosci. 2020; 7. https://doi.org/10.3389/fmolb.2020.586540

Shinoda W, DeVane R, Klein ML. Zwitterionic Lipid Assemblies: Molecular Dynamics Studies of Monolayers, Bilayers, and Vesicles Using a New Coarse Grain Force Field. J Phys Chem B. 2010 May; 114(20):6836–6849. https://doi.org/10.1021/jp9107206

Silhavy TJ, Kahne D, Walker S. The bacterial cell envelope. Cold Spring Harb Perspect Biol. 2010 May; 2(5):a000414. https://doi.org/10.1101/cshperspect.a000414

Smart OS, Neduvelil JG, Wang X, Wallace BA, Sansom MSP. HOLE: A program for the analysis of the pore dimensions of ion channel structural models. J Molec Graphics. 1996 Dec; 14(6):354–360. https://doi.org/10.1016/S0263-7855(97)00009-X

Sodt AJ, Sandar ML, Gawrisch K, Pastor RW, Lyman E. The Molecular Structure of the Liquid-Ordered Phase of Lipid Bilayers. J Am Chem Soc. 2014 Jan; 136(2):725–732. https://doi.org/10.1021/ja4105667

Sohlenkamp C, Geiger O. Bacterial membrane lipids: diversity in structures and pathways. FEMS Microbiol Rev. 2016 Jan; 40(1):133–159. https://doi.org/10.1093/femsre/fuv008

Song C, de Groot BL, Sansom MSP. Lipid Bilayer Composition Influences the Activity of the Antimicrobial Peptide Dermcidin Channel. Biophys J. 2019 May; 116(9):1658–1666. https://doi.org/10.1016/j.bpj.2019.03.033

Sun D, Forsman J, Woodward CE. Multistep Molecular Dynamics Simulations Identify the Highly Cooperative Activity of Melittin in Recognizing and Stabilizing Membrane Pores. Langmuir. 2015 Sep; 31(34):9388–9401. https://doi.org/10.1021/acs.langmuir.5b01995

Sun L, Wang S, Tian F, Zhu H, Dai L. Organizations of melittin peptides after spontaneous penetration into cell membranes. Biophys J. 2022 Nov; 121(22):4368–4381. https://doi.org/10.1016/j.bpj.2022.10.002

Sun Y, Deng Z, Jiang X, Yuan B, Yang K. Interactions between polymyxin B and various bacterial membrane mimics: A molecular dynamics study. Colloids Surf B: Biointerfaces. 2022 Mar; 211:112288. https://doi.org/10.1016/j.colsurfb.2021.112288

Ulmschneider JP. Charged Antimicrobial Peptides Can Translocate across Membranes without Forming Channel-like Pores. Biophysical J. 2017 Jul; 113(1):73–81. https://doi.org/10.1016/j.bpj.2017.04.056

Ulmschneider JP, Smith JC, White SH, Ulmschneider MB. In Silico Partitioning and Transmembrane Insertion of Hydrophobic Peptides under Equilibrium Conditions. J Am Chem Soc. 2011 Oct; 133(39):15487–15495. https://doi.org/10.1021/ja204042f

Ulmschneider MB, Doux JPF, Killian JA, Smith JC, Ulmschneider JP. Mechanism and Kinetics of Peptide Partitioning into Membranes from All-Atom Simulations of Thermostable Peptides. J Am Chem Soc. 2010 Mar; 132(10):3452–3460. https://doi.org/10.1021/ja909347x

Ulmschneider MB, Ulmschneider JP, Schiller N, Wallace BA, von Heijne G, White SH. Spontaneous transmembrane helix insertion thermodynamically mimics translocon-guided insertion. Nature Commun. 2014 Sep; 5(1):4863. https://doi.org/10.1038/ncomms5863

Vaiwala R, Ayappa KG. Martini-3 Coarse-Grained Models for the Bacterial Lipopolysaccharide Outer Membrane of Escherichia coli. J Chem Theory Comput. 2024 Feb; 20(4):1704–1716. https://doi.org/10.1021/acs.jctc.3c00471

Venable RM, Krämer A, Pastor RW. Molecular Dynamics Simulations of Membrane Permeability. Chem Rev. 2019 May; 119(9):5954–5997. https://doi.org/10.1021/acs.chemrev.8b00486

Vesentini S, Soncini M, Zaupa A, Silvestri V, Fiore GB, Redaelli A. Multi-Scale Analysis of the Toraymyxin Adsorption Cartridge Part I: Molecular Interaction of Polymyxin B with Endotoxins. Int J Artif Organs. 2006 Feb; 29(2):239–250. https://doi.org/10.1177/039139880602900210

Wang Y, Chen CH, Hu D, Ulmschneider MB, Ulmschneider JP. Spontaneous formation of structurally diverse membrane channel architectures from a single antimicrobial peptide. Nature Commun. 2016 Nov; 7(1):13535. https://doi.org/10.1038/ncomms13535

Wang Y, Markwick PRL, de Oliveira CAF, McCammon JA. Enhanced Lipid Diffusion and Mixing in Accelerated Molecular Dynamics. J Chem Theory Comput. 2011 Oct; 7(10):3199–3207. https://doi.org/10.1021/ct200430c

Wang Y, Schlamadinger DE, Kim JE, McCammon JA. Comparative molecular dynamics simulations of the antimicrobial peptide CM15 in model lipid bilayers. Biochimica et Biophysica Acta (BBA) - Biomembranes. 2012 May; 1818(5):1402–1409. https://doi.org/10.1016/j.bbamem.2012.02.017

Wang Y, Zhao T, Wei D, Strandberg E, Ulrich AS, Ulmschneider JP. How reliable are molecular dynamics simulations of membrane active antimicrobial peptides? Biochimica et Biophysica Acta (BBA) - Biomembranes. 2014 Sep; 1838(9):2280–2288. https://doi.org/10.1016/j.bbamem.2014.04.009

Wassenaar TA, Ingólfsson HI, Böckmann RA, Tieleman DP, Marrink SJ. Computational Lipidomics with insane: A Versatile Tool for Generating Custom Membranes for Molecular Simulations. J Chem Theory Comput. 2015 May; 11(5):2144–2155. https://doi.org/10.1021/acs.jctc.5b00209

Willdigg JR, Helmann JD. Mini Review: Bacterial Membrane Composition and Its Modulation in Response to Stress. Fronti Molec Biosci. 2021; 8. https://doi.org/10.3389/fmolb.2021.634438

Wimley WC. Describing the Mechanism of Antimicrobial Peptide Action with the Interfacial Activity Model. ACS Chem Biol. 2010 Oct; 5(10):905–917. https://doi.org/10.1021/cb1001558

World Health Organization. Ten threats to global health in 2019 [Internet]. [cited March 29, 2023]. Available from: https://www.who.int/news-room/spotlight/ten-threats-to-global-health-in-2019

Yesylevskyy S, Khandelia H. EnCurv: Simple Technique of Maintaining Global Membrane Curvature in Molecular Dynamics Simulations. J Chem Theory Comput. 2021 Feb; 17(2):1181–1193. https://doi.org/10.1021/acs.jctc.0c00800

Yesylevskyy SO, Ramseyer C. Determination of mean and Gaussian curvatures of highly curved asymmetric lipid bilayers: the case study of the influence of cholesterol on the membrane shape. Phys Chem Chem Phys. 2014; 16(32):17052–17061. https://doi.org/10.1039/C4CP01544D

Yesylevskyy SO, Schäfer LV, Sengupta D, Marrink SJ. Polarizable Water Model for the Coarse-Grained MARTINI Force Field. PLOS Comput Biol. 2010 Jun; 6(6):e1000810. https://doi.org/10.1371/journal.pcbi.1000810

Yoo J, Winogradoff D, Aksimentiev A. Molecular dynamics simulations of DNA–DNA and DNA–protein interactions. Curr Opinion Structural Biol. 2020 Oct; 64:88–96. https://doi.org/10.1016/j.sbi.2020.06.007

Zakharova AA, Efimova SS, Ostroumova OS. Lipid Microenvironment Modulates the Pore-Forming Ability of Polymyxin B. Antibiotics. 2022; 11(10). https://doi.org/10.3390/antibiotics11101445

Zasloff M. Antimicrobial peptides of multicellular organisms. Nature. 2002 Jan; 415(6870):389–395. https://doi.org/10.1038/415389a

Zhao L, Cao Z, Bian Y, Hu G, Wang J, Zhou Y. Molecular Dynamics Simulations of Human Antimicrobial Peptide LL-37 in Model POPC and POPG Lipid Bilayers. Int J Molec Sci. 2018; 19(4). https://doi.org/10.3390/ijms19041186

APPENDIX

Table of Acronyms Used in the Review Paper

AA	All-atom
AMBER	Assisted Model Building with Energy Refinement
AMP	Antimicrobial peptide
AMR	Antimicrobial resistance
APL	Area per lipid
CG	Coarse-grained
CHARMM	Chemistry at HARvard Macromolecular Mechanics
CL	Cardiolipin
COM	Center-of-mass
CPP	Cell-penetrating peptide
CV	Collective variable
DAB	α, γ-diamino butyric acid
DNA	Deoxyribonucleic acid
DPPE	Diplamitoylphosphatidylethanolamine
DPPG	Diplamitoylphosphatidylglycerol
ELBA	ELectrostatic-BAsed
ESKAPE	*Enterococcus faecium, Staphylococcus aureus, Klebsiella pneumoniae, Acetinobacter baumannii, Pseudomonas aeruginosa,* and *Enterobacter spp.*
GROMOS	GROningen MOlecular Simulation
IM	Inner membrane
KDO	3-deoxy-D-manno-2-octulosonic acid
LPS	Lipopolysaccharide
MD	Molecular dynamics
OM	Outer membrane
OPLS	Optimized Potentials for Liquid Simulations
PE	Phosphatidylethanolamine
PG	Phosphatidylglycerol
PmB	Polymyxin B
PMF	Potential mean force
POPC	Palmitoyloleoylphosphatidylethanolamine
POPG	Palmitoyloleoylphosphatidylglycerol
SDK	Shinoda-DeVane-Klein
UA	United-atom